Available online at www.sciencedirect.com

ScienceDirect

IFAC PapersOnline CONFERENCE PAPER ARCHIVE

IFAC PapersOnLine 53-2 (2020) 10052–10057

Combined Joint-Cartesian Mapping for Simultaneous Shape and Precision Teleoperation of Anthropomorphic Robotic Hands

R. Meattini, D. Chiaravalli, L. Biagiotti, G. Palli and C. Melchiorri

Dept. of Electrical, Electronic and Information Engineering (DEI) University of Bologna, Viale del Risorgimento 2, 40136 Bologna, Italy (e-mail: roberto.meattini2@unibo.it).

Abstract: There are many applications involving robotic hands in which teleoperation-based approaches are preferred to autonomous solutions. The main reason is that cognitive skills of human operators are desirable in some task scenarios, in order to overcome limitations of robotic hands abilities in dealing with unstructured environments and/or unpredetermined requirements. In particular, in this work we focus on the use of anthropomorphic grasping devices and, specifically, on their teleoperation based on movements of the human operator's hand (the master hand.) Indeed, the mapping of human hand configurations to an anthropomorphic robotic hand (the slave device) is still an open problem, because of the presence of dissimilar kinematics between master and slave that produce shape and/or Cartesian errors – as addressed within our study. In this work, we propose a novel algorithm that combines joint and Cartesian mappings in order to enhance the preservation of both finger shapes and fingertip positions during the teleoperation of the robotic hand. In particular, a transition between the joint and Cartesian mappings is realized on the basis of the distance between the fingertip of the master hands' thumb and the opposite fingers, in which the mapping of the thumb fingertip is specifically addressed. The result of the testing of the algorithm with a ROS-based simulator of a commercially available robotic hand is reported, showing the effectiveness of the proposed mapping.

Keywords: Anthropomorphic Robotic Hand, Teleoperation, Joint, Cartesian, Mapping.

1. INTRODUCTION

When unstructured environments and a large variety of objects and actions are present in a task scenario, often autonomous manipulation approaches give way to *human-in-the-loop* controls (Meattini et al., 2018), i.e. to telemanipulation applications in which the interface between the human operator (*master*) and the robotic hand (*slave device*) plays a fundamental role. It is therefore important, that intuitive communication, ease of use and good reproducibility of master's hand motions on the slave device are matched, in order to increase the so called *human operability* (Bicchi, 2000).However telemanipulation based on human hand motions requires a mapping between teleoperator's and robot's finger motions, which is far from being straightforward because of the presence of dissimilar kinematics between the *master* and *slave hand*. Indeed, when dissimilar kinematics are involved, it is not possible to exactly replicate the motions of the master hand's phalanges on the slave finger's links; on the other hand, it is certainly important to preserve the intuitiveness of the control interface (Meeker et al., 2018). To this purpose, it is fundamental that two aspects are taken into account: (*i*) the reproduction of the shape of the master hand onto the slave hand – in terms of joint mapping – which enables reproducing gestures and predicting future motions by just looking at the grasping device (Meeker et al., 2018), and (*ii*) the replication on the slave hand of the coordination between the thumb and other finger fingertips – in terms of Cartesian mapping – in order to preserve precision teleoperation skills and prehensile performance. In literature, several approaches have been presented for the mapping of the human hand to an anthropomorphic grasping device, which can be mainly classified into direct joint mapping (Liarokapis et al., 2013) and mapping of the fingertip Cartesian position (Gioioso et al., 2013). In joint mapping approaches, the master hand's joint angles are directly imposed onto the robotic hand. This approach ensures only similarities of the hand shapes, and therefore is appropriate for the execution of gestures and power grasps (Cerulo et al., 2017). When precision is required, fingertip mapping is normally adopted, in which a correspondence between the master and slave Cartesian fingertips positions is implemented. Although this method allows to achieve precise motions of the fingertips, it results counterintuitive for the operator when the replication of the hand shape is important and in general if master and slave workspaces present significant differences (Gioioso et al., 2013). In hybrid mappings, different approaches are merged together to improve the performance of the teleoperation system.

10.1016/j.ifacol.2020.12.2726

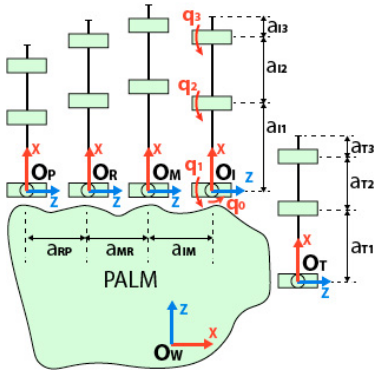

Fig. 1. Kinematic model of the master and slave hands.

These methods try to increase the intuitiveness of control for the operator and have proved to be effective in grasping operations (Colasanto et al., 2012). At the same time, no studies have taken into account the preservation – on the robotic hand – of the distance between the master hand's thumb and finger fingertips when a precise teleoperation is desired by the operator. Instead, such an aspect is essential in almost the totality of the activities that require an accurate positioning of the hand fingertips (Kuo et al., 2009) and – we claim – for the overall sense of controllability, and even embodiment (Paulos and Canny, 1998) of the teleoperated grasping device. In the light of these concepts, in this work we propose a novel master-to-slave mapping algorithm for enhancing the intuitiveness in the teleoperation of anthropomorphic robotic hands, by combining both joint and Cartesian hand mappings. In particular, the proposed algorithm is based on the distance between the thumb and finger fingertips on the master side in order to preserved both the shape and the thumb-finger fingertips distance. Additionally, other important aspects in the design of the algorithm are the transition between the joint and Cartesian mappings on the robotic hand, and the Cartesian mapping of the thumb fingertip. In the article, the algorithm is illustrated in detail and simulation experiments using a ROS-based simulator of the commercially available Allegro Hand are reported in order to show the effectiveness of the proposed solution.
The article is organized as follows: in Sec. 2 the teleoperation shape and Cartesian errors are introduced, and the proposed mapping algorithm is illustrated; Sec. 3 reports the results of simulation experiments and Sec. 4 outlines conclusions and future work directions.

2. METHODS

2.1 Master and Slave Hand

In order to describe the mapping algorithm of the present work, let us consider a master and slave hand modelled as depicted in Fig. 1. They have the same kinematic structure with $n = 20$ DoFs but with different sizes. In particular the master device corresponds to the *paradigmatic hand* model (Gabiccini et al., 2011), which is a model representing a trade-off between the complexity of the human hand model and the simplicity and accessibility of the models of the robotic hands available (Palli et al., 2012). It is assumed that the motions of the master hand of Fig. 1 exactly coincides with the real motions of a human operator hand during the teleoperation of a robotic hand, since the focus of the present work is on the master-to-slave mapping function, whereas the (open) problem of correctly measuring human hand motions lies outside of the article aims. Also in accordance with the notation reported in Fig. 1, we here describe in detail only the index finger model of the master hand, since all the fingers present the same kinematic structure. The kinematic chain of the index is composed by 4 DoFs, which are: adduction/abduction (q_0), metacarpal (q_1), proximal interphalangeal (q_2) and distal interphalangeal (q_3). Setting a_{I1}, a_{I2} and a_{I3} the phalanx lengths of the master hand index, we consider the corresponding lengths of the slave index, a_{SI1}, a_{SI2} and a_{SI3}, such that the relation $a_{SI1}+a_{SI2}+a_{SI3} \geq a_{I1}+a_{I2}+a_{I3}$ holds – this is extended for all the pairs of master-slave hand fingers. In particular, the dissimilarities between the master and slave phalanx lengths generate – during the teleoperation – a *shape* and/or *Cartesian error* on the slave side, as discussed in the next subsection.

2.2 Shape and Cartesian Error

A teleoperation mapping $\mathcal{M}(\cdot)$ is usually defined as a mathematical relation from a vector describing the master motion and a vector describing the slave one. Given a certain joint *configuration* $q \in \mathbb{R}^n$ of the master device, a *joint mapping* $\mathcal{M}_Q(\cdot) : \mathbb{R}^n \to \mathbb{R}^m$ is defined as an isomorphism between the joint spaces of the two hands according to

$$q_S = \mathcal{M}_Q(q). \tag{1}$$

Differently, given a master hand and a slave hand with the number of fingers equal to v and g, respectively, a *Cartesian mapping* $\mathcal{M}_C(\cdot) : \mathbb{R}^{3v} \to \mathbb{R}^{3g}$ is an isomorphism such that

$$p_{SF} = \mathcal{M}_C(p_F), \tag{2}$$

where $p_F = [{}^{O_T}p_T^T \ \dots \ {}^{O_i}p_i^T \ \dots \ {}^{O_P}p_P^T]^T \in \mathbb{R}^{15}$ and $p_{SF} = [{}^{O_{ST}}p_{ST}^T \ \dots \ {}^{O_{Si}}p_{Si}^T \ \dots \ {}^{O_{SP}}p_{SP}^T]^T \in \mathbb{R}^{15}$ are the fingertip positions of the master and slave hands, respectively. These two position vector are evaluated with respect to the frames $\{O_i\}$ and $\{O_{Si}\}$, and with $i = \{T, I, M, R, P\}$ denoting the thumb, index, middle, ring and pinkie fingers. Furthermore, in this control framework, we define a Cartesian error e_C described as

$$e_C = \|p_F - p_{SF}\|, \tag{3}$$

and a shape error e_Q such that

$$e_Q = \|q - q_S\|. \tag{4}$$

In Fig. 2 the shape and Cartesian error values are plotted for the index finger only, as a function of the phalanx lengths of the slave, by uniformly discretizing the space $\{a_{SI1}, a_{SI2}, a_{SI3}\}$, subjects to $a_{SI1} + a_{SI2} + a_{SI3} \geq a_{I1} + a_{I2} + a_{I3}$ and 10 mm $\leq a_{SI1}, a_{SI2}, a_{SI3} \leq 50$ mm, while the values a_{I1}, a_{I2}, a_{I3} of the master are constant as reported in Tab. 1. In particular Fig. 2a reports the shape error for the slave hand's index joints q_{S2} when a Cartesian mapping of the type

$${}^{O_{SI}}p_{SI} = {}^{O_I}p_I \tag{5}$$

is implemented, where ${}^{O_I}p_I$ and ${}^{O_{SI}}p_{SI}$ are the master and slave index fingertip positions, respectively. Dually, Fig. 2b reports the Cartesian error of the slave hand's index fingertip positions along the main finger motion direction when a joint mapping of the type

$$q_{SI} = q_I \tag{6}$$

is set, where $q_I = [q_0 \ q_1 \ q_2 \ q_3]^T$ and $q_{SI} = [q_{S0} \ q_{S1} \ q_{S2} \ q_{S3}]^T$ are the master and slave index joint angles, respectively.

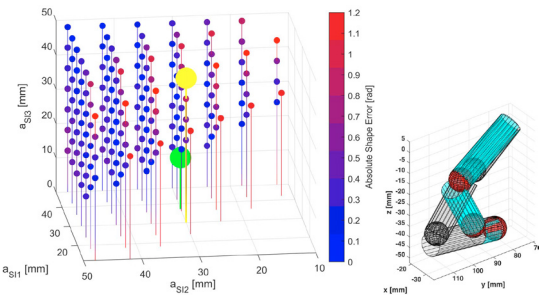

(a) Left: index shape error for the joint q_{2S}; right: combination of a_{S1}, a_{S2}, a_{S3} producing the maximum shape error along q_{S2} (colored finger: master; transparent finger: slave.)

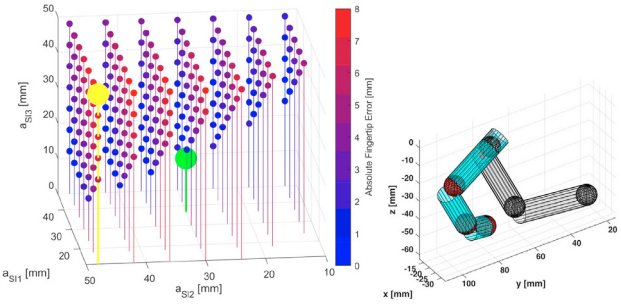

(b) Left: index Cartesian error for the y dimension; right: combination of $a_{SI1}, a_{SI2}, a_{SI3}$ producing the maximum Cartesian error along y (colored finger: master; transparent finger: slave.).

Fig. 2. Representation of the shape and Cartesian errors as a function of the phalanx lengths of the slave hand, considering a discretization of the space of $\{a_{SI1}, a_{SI2}, a_{SI3}\}$ combinations – refer to Fig. 1, with Cartesian mapping (a) and joint mapping (b). In the 3-D graphs, the yellow and green circles indicate the maximum and minimum errors, respectively, for the relative joint or Cartesian dimension.

Eq. (5) and (6) can be easily applied for all the fingers, therefore extending the qualitative characterization of Fig. 2 to the entire hand. To summarize, if a "Cartesian-only" mapping as in eq. (5) is implemented for the teleoperation of a robotic hand, it is possible to perform a precise fingertip control of the slave device (i.e., $e_C = 0$), but, in turn, it will introduce a shape error e_Q affecting intuitiveness and execution of gestures; on the other hand, if a pure joint mapping is realized, the hand shape will be preserved ($e_Q = 0$), but at the cost of a Cartesian error e_C.

2.3 Proposed Hand Mapping Algorithm

During precise actions, the fingers' fingertips operate very close in space to the thumb endpoint. Therefore when the module of the vector of the master thumb-finger fingertips distance is lower than a certain threshold value, a controlled transition is enforced from the joint mapping to the Cartesian mapping. Additionally, since during the Cartesian mapping we want to preserve the relative (scaled) distances between the master hands' thumb and involved fingertips, these latter will be mapped with respect to the thumb fingertip; in turn, the thumb fingertip will be mapped by referring to the frames $\{O_i\}$ and $\{O_{Si}\}$, with $i = \{T, I, M, R, P\}$, as explained in the following section.

Joint-Cartesian Algorithm and Switching Condition Let us consider the subscript $j = \{I, M, R, P\}$ such that ${}^{Ow}p_j$ indicates the fingertip position for the master hands' index, middle, ring and pinkie fingers and ${}^{Ow}p_T$ the position for the master's thumb fingertip, with respect to the frame $\{O_W\}$ (see Fig. 1.) Let r_1 be the radius of a sphere centered in ${}^{Ow}p_T$. When the inequality $\|{}^{Ow}p_T - {}^{Ow}p_j\| > r_1$ is satisfied for all fingers, then we set the master-to-slave hand mapping as given by

$$q_S = q, \tag{7}$$

i.e., a joint mapping is implemented for the teleoperation of the robotic hand . Otherwise, if the switching condition

$$\|{}^{Ow}p_T - {}^{Ow}p_h\| \leq r_1, \tag{8}$$

is matched for at least one finger, with $h \subset \{I, M, R, P\}$ such that ${}^{Ow}p_h$ represents the master hands' fingertip position for the only fingers that satisfy Eq. (8), then the mapping is switched to Cartesian, and is implemented as

$${}^{OsW}p_{Sh} = c_s({}^{Ow}p_h - {}^{Ow}p_T) + {}^{OsW}p_{ST}, \tag{9}$$

where ${}^{OsW}p_{Sh}$ represents the slave hands' fingertip positions for the fingers that satisfy Eq. (8), ${}^{OsW}p_{ST}$ is the slave hands' thumb fingertip position and c_s is a scaling constant set as $c_s = (a_{ST1} + a_{ST2} + a_{ST3})/(a_{T1} + a_{T2} + a_{T3})$. In other words, according to Eq. (9), the master's fingertips whose position is within a sphere with radius r_1 and centered in the thumb fingertip, are mapped in the robotic hand based on their relative position with respect to the master's thumb fingertip itself. The slave hand's thumb, in turn – if at least one finger satisfies Eq. (8) – is controlled according to a different Cartesian mapping, which is reported here in the following. By taking into account the master and slave hands' fingertip positions in terms of their x, y and z components, we can consider: ${}^{Ow}p_i = [{}^{Ow}p_{ix}^T \ {}^{Ow}p_{iy}^T \ {}^{Ow}p_{iz}^T]^T$ and ${}^{OsW}p_{Si} = [{}^{OsW}p_{Six}^T \ {}^{OsW}p_{Siy}^T \ {}^{OsW}p_{Siz}^T]^T$, with $i = \{T, I, M, R, P\}$. Let us therefore define

$$d_{\{l,t\}} = \frac{\|{}^{OsW}p_{O_{St}x} - {}^{OsW}p_{O_{Sl}x}\|}{\|{}^{Ow}p_{O_tx} - {}^{Ow}p_{O_lx}\|}$$

and the thumb position relative to frame of finger m:

$$\tilde{p}_m = {}^{Ow}p_T - {}^{Ow}p_{O_m},$$

where the subscripts l, t and m are given according to $\{l,t\} = \{\{I,M\},\{M,R\},\{R,P\}\}$ and $m = \{I, M, R\}$. The Cartesian mapping for the robotic hand thumb is given, for its x component, as

$${}^{OsW}p_{STx} = \tag{10}$$

$$= \begin{cases} {}^{OsW}p_{STx_1}, & \text{if } {}^{Ow}p_{Tx} \geq {}^{Ow}p_{O_Ix} \\ {}^{OsW}p_{STx_2}, & \text{if } {}^{Ow}p_{O_Mx} < {}^{Ow}p_{Tx} \leq {}^{Ow}p_{O_Ix} \\ {}^{OsW}p_{STx_3}, & \text{if } {}^{Ow}p_{O_Rx} < {}^{Ow}p_{Tx} \leq {}^{Ow}p_{O_Mx} \\ {}^{OsW}p_{STx_4}, & \text{if } {}^{Ow}p_{O_Px} < {}^{Ow}p_{Tx} \leq {}^{Ow}p_{O_Rx} \\ {}^{OsW}p_{STx_5}, & \text{if } {}^{Ow}p_{Tx} < {}^{Ow}p_{O_Px}, \end{cases}$$

where

$$\begin{aligned} {}^{OsW}p_{STx_1} &= [{}^{OsW}T_{O_{SI}} {}^{O_I}p_{Tx} c_s]_x, \\ {}^{OsW}p_{STx_2} &= {}^{OsW}T_{O_{SI_x}} + d_{\{I,M\}}[\tilde{p}_I]_x, \\ {}^{OsW}p_{STx_3} &= {}^{OsW}T_{O_{SM_x}} + d_{\{M,R\}}[\tilde{p}_M]_x, \\ {}^{OsW}p_{STx_4} &= {}^{OsW}T_{O_{SR_x}} + d_{\{R,P\}}[\tilde{p}_R]_x, \\ {}^{OsW}p_{STx_5} &= [{}^{OsW}T_{O_{SP}} {}^{O_P}p_{Tx} c_s]_x; \end{aligned}$$

whereas, for the y and z components:

$${}^{OsW}p_{STy} = [{}^{OsW}T_{O_{SI}} {}^{O_I}p_{Ty} c_s]_y \tag{11}$$

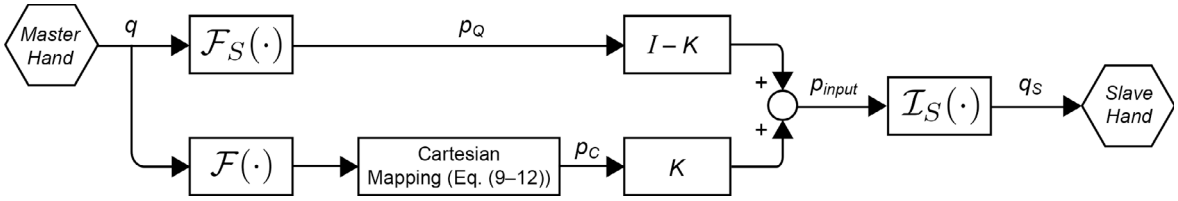

Fig. 3. Block diagram of the algorithm based on the combined joint-Cartesian mapping illustrated in Subsec. 2.3.

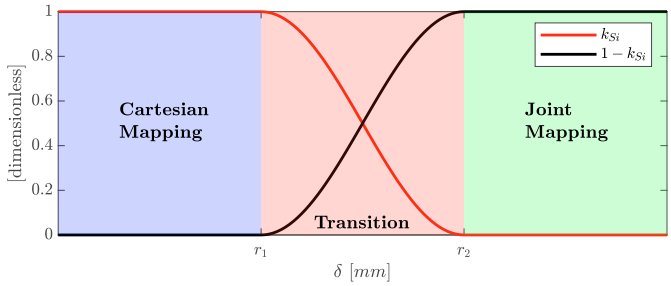

Fig. 4. Spatial behaviour of the components $1 - k_{Si}$ and k_{Si} of the matrices $(I - K)$ and K, respectively.

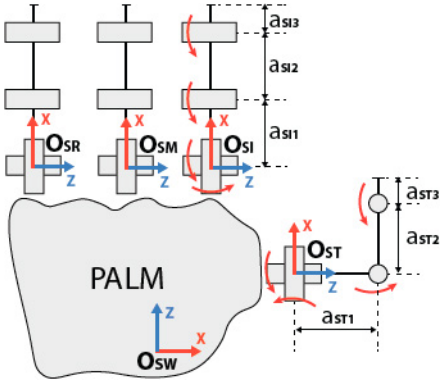

Fig. 5. Kinematic structure of the Allegro Hand used as slave hand .

and

$$ {}^{O_{SW}}p_{STz} = [{}^{O_{SW}}T_{O_{SI}}\,{}^{O_I}p_T c_s]_z \tag{12}$$

In the proposed equations the formulation $[h]_i$ denotes the component along the i axis of the vector h. Note that ${}^{O_{SW}}T_{O_{Si}}$, with $i = \{T, I, M, R, P\}$, represents the homogeneous linear transformation that describes the frame $\{O_{Si}\}$ with respect to the frame $\{O_{SW}\}$. In this way, according to Eq. (10), (11) and (12), we obtain a Cartesian mapping of the thumb such that the distance between the master hands' thumb fingertip – along the x component – and the base frame origins of the other fingers (along the x component) is preserved – in scale – on the slave hand; differently, the mapping of the thumb y and z components are instead arbitrarily implemented on the basis of the distance between the master's thumb fingertip and the origin of the frame $\{O_I\}$.

Joint-Cartesian Transition and Online Algorithm A smooth transition is defined between the two type of teleoperation controls, in order to avoid discontinuities in the master-slave interfacing. We will refer to $\mathcal{F}(\cdot)$, $\mathcal{F}_S(\cdot)$ as the forward kinematic functions for the master and slave hands and to $\mathcal{I}(\cdot)$, $\mathcal{I}_S(\cdot)$ as the inverse kinematic functions for the master and slave hands, respectively. Let us consider p_Q the Cartesian position of the slave hand's fingertips

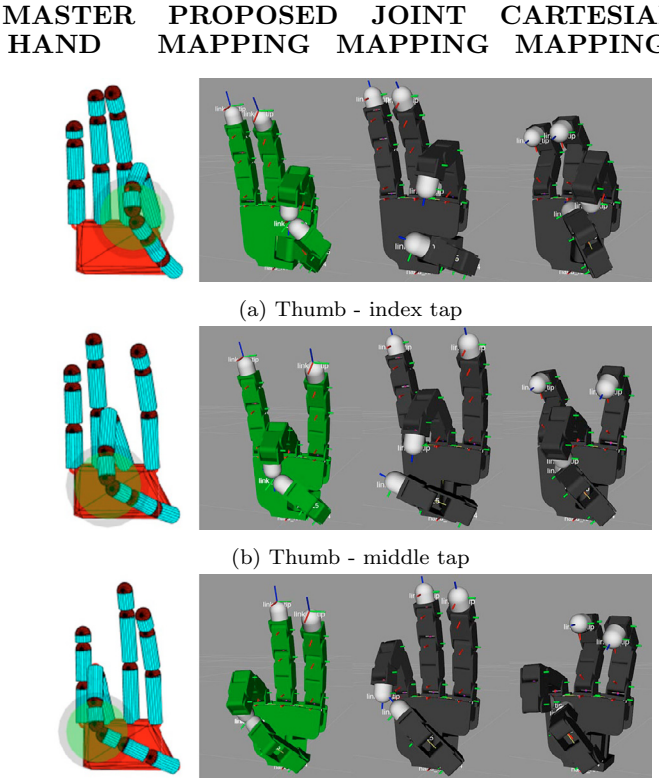

(a) Thumb - index tap

(b) Thumb - middle tap

(c) Thumb - ring tap

Fig. 6. Mapping on the Allegro Hand of thumb-finger tapping gestures.

according to the joint mapping (Eq. (7)), i.e., $p_Q = \mathcal{F}_S(q)$, and p_C the Cartesian position *according to the Cartesian mapping*, i.e., Eq. (9)—(12). Furthermore, we refer to p_{input} as the actual input that we provide to control the robotic hand (which will be then converted to an input in the joint space according to $q_S = \mathcal{I}_S(p_{input})$, see Fig. 3). To the purpose of implementing the transition between p_Q and p_C during a continuous online teleoperation of the robotic hand, we set

$$ p_{input} = (I - K)\,p_Q + K\,p_C, \tag{13}$$

where I is a 15×15 identity matrix and

$$ K = \mathrm{diag}(\underbrace{k_{ST}, ..., k_{ST}}_{3\text{ times}}, ..., \underbrace{k_{Si}, ..., k_{Si}}_{3\text{ times}}, ..., \underbrace{k_{SP}, ..., k_{SP}}_{3\text{ times}}), $$

with $i = \{T, I, M, R, P\}$ denoting the different robotic hand fingers, and in which k_{Si} is a nonlinear, smooth gain described by

$$ k_{Si}(\delta_i) = \begin{cases} 1 & \text{if } \delta < r_1 \\ \frac{1}{2}(1 + cos(\frac{\delta_i \pi}{r_2 - r_1})) & \text{if } r_1 \leq \delta_i \leq r_2 \\ 0, & \text{if } \delta_i > r_2, \end{cases} \tag{14}$$

where $\delta_i = \|{}^{Ow}p_T - {}^{Ow}p_i\|$, with $i = \{I, M, R, P\}$. The gain K_{ST} defines the thumb dynamic and is always

Table 1. Master and Slave hand dimensions.

Paradigmatic Hand						**Allegro Hand**				
Phalanx	T	I	M	R	P	**Phalanx**	T	I	M	R
a_{i1} $[mm]$	25	37	40	37	27	a_{Si1} $[mm]$	57	54	54	54
a_{i2} $[mm]$	20	30	35	30	25	a_{Si2} $[mm]$	51	38	38	38
a_{i3} $[mm]$	15	15	17	15	10	a_{Si3} $[mm]$	54	38	38	38

equal to the gain of the closest finger j. Note that Eq. (13) implements a smooth transition from p_Q to p_C, and viceversa, according to a spatial sigmoid-like profile. Specifically, such sigmoid-like profile acts when a master hands' fingertip is located in the area comprised between the surfaces of two spheres centered in the thumb fingertip with radius r_1 and r_2 ($r_2 > r_1$), as illustrated in Fig. 4. The radius r_1 and r_2 act as a tradeoff between shape and precision control. Their definition is dependent on the task characteristics and hand dimensions: gesture execution could require precise contact only on the finger tips and therefore a reduced sphere; on the other hand object grasping would require an increase in the dimension of cartesian mapping and a bigger radius r_1.

3. SIMULATION AND RESULTS

In order to test the algorithm illustrated in Sec. 2, we performed a simulation experiment in which a set of gestures and motions of a master hand have been mapped into a simulated slave robotic hand. As master hand we used the paradigmatic hand model, whose simulation has been performed by using the open-source SynGrasp Matlab toolbox (Malvezzi et al., 2015), see Fig. 6. On the other hand, as slave robotic hand, for this test we used the simulator of the commercially available Allegro Hand (WonikRobotics, 2015). The Allegro Hand simulator is implemented in ROS and tracked on Rviz, the Ros visualization platform. Indeed, it is an anthropomorphic grasping device with a kinematic structure slightly different from the model of the paradigmatic hand (see Fig. 5), therefore giving the possibility to preliminary test the generalizability of the mapping algorithm for slave hands that don't exactly reproduce the kinematics considered in Fig. 1. Furthermore, the phalanx lengths of the Allegro Hand are clearly longer than standard human phalanges,well spreading the shape and Cartesian errors illustrated in Fig. 2, and therefore making this robotic hand a likely real case of a commercial device on which a user can benefit from the proposed teleoperation mapping. Fig. 6 reports the master-to-slave mapping of three "thumb-to-finger tapping" gestures, i.e., specifically, the hand configurations resulting from bringing in contact the thumb-index, thumb-middle and thumb-ring fingertips. As it is possible to observe from the simulation results of Fig. 6, the master hand gestures were reproduced more faithfully by the proposed mapping algorithm with respect to the joint-only and Cartesian-only mappings, the latter two introducing shape and Cartesian errors in the robotic hand The reason of this is thatthe cartesian mapping is applied only to the slave fingers whose related master hands' fingertips enter within a sphere centered in the thumb fingertip, i.e.: the green sphere in Fig. 6, corresponding to the sphere with radius r_1 in Subsec. 2.3. Note that the grey sphere in Fig. 6 corresponds to the sphere with radius r_2 in Subsec. 2.3, used to implement the smooth transition between joint and Cartesian mappings. Indeed, this last aspect is more clearly shown in Fig. 8, where the signals involved in the mapping of a tripodal motion on the Allegro Hand (see its visualization in Fig. 7) are reported. In relation to such figure, it can be easily appreciated the switching between the Cartesian reference p_Q produced by the joint mapping (blue dotted line) and the Cartesian reference p_C provided by the Cartesian mapping (black dotted line) – also refer to Fig. 3. Furthermore, it is clearly observable the presence of the sigmoid-like transition, that for the thumb is located around $t = 30s$ (closure motion) and around $t = 50s$ (opening motion). Note that the transition for the index finger occurs at the same time instants, since the mapping starts by these two specific fingers. Differently, the transitions for the middle finger take place at different time instants, due to the distance with respect to the thumb end-tip that is less than r_2 in a desynchronized manner with respect to the index finger. Eventually the plots of the bottom two rows of Fig. 8 report for the related values of K (see Fig. 3) and of the shape and Cartesian errors, which are equal to zero in the related "joint-only" and "Cartesian-only" phases of the proposed mapping algorithm.

4. CONCLUSIONS

In this paper a novel mapping strategy for the teleoperation of anthropomorphic hands by means of human hand motions has been presented. In particular, the proposed algorithm exploits a combination of joint and Cartesian mappings in order to preserve both shape and precise fingertips teleoperation for the operator. Simulation experiments have been carried out, in which key master hand configurations and continuous motions were mapped onto a ROS-based simulator of the commercially available Allegro Hand. The results show that the proposed mapping effectively allows to perform simultaneous shape and fingertips control for different fingers, reporting also for the consistency of the transition between the joint/Cartesian control spaces. Future work will be devoted to take into account also grasp activities and gesture mimicry produced by a human operator interacting with a real scenario, also producing experimental results using a real robotic hand.

REFERENCES

Bicchi, A. (2000). Hands for dexterous manipulation and robust grasping: A difficult road toward simplicity. *IEEE Transactions on robotics and automation*, 16(6), 652–662.

Cerulo, I., Ficuciello, F., Lippiello, V., and Siciliano, B. (2017). Teleoperation of the schunk s5fh under-actuated anthropomorphic hand using human hand motion tracking. *Robotics and Autonomous Systems*, 89, 75–84.

Colasanto, L., Suárez, R., and Rosell, J. (2012). Hybrid mapping for the assistance of teleoperated grasping tasks. *IEEE Transactions on Systems, Man, and Cybernetics: Systems*, 43(2), 390–401.

Gabiccini, M., Bicchi, A., Prattichizzo, D., and Malvezzi, M. (2011). On the role of hand synergies in the optimal choice of grasping forces. *Autonomous Robots*, 31(2-3), 235.

Gioioso, G., Salvietti, G., Malvezzi, M., and Prattichizzo, D. (2013). Mapping synergies from human to robotic

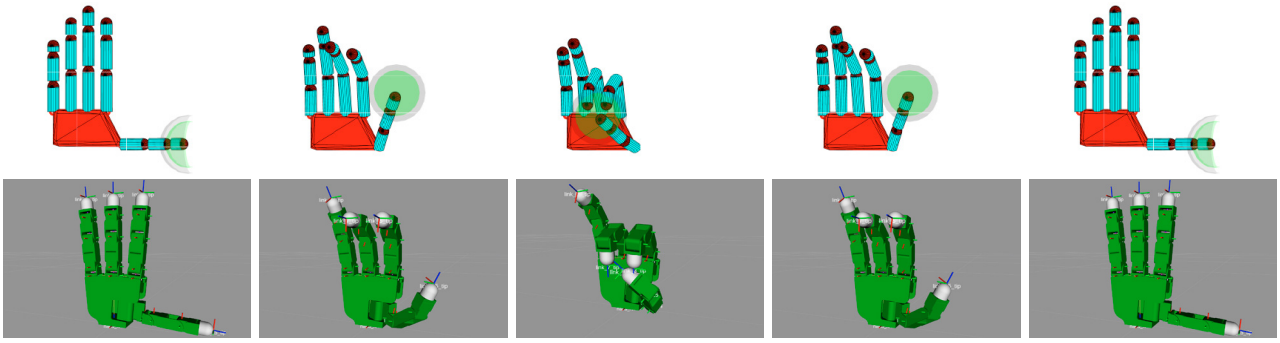

(a) $t = 0s$ in Fig. 8. (b) $t = 2s$ in Fig. 8. (c) $t = 4s$ in Fig. 8. (d) $t = 6s$ in Fig. 8. (e) $t = 8s$ in Fig. 8.

Fig. 7. Visual frames of the master hand and the Allegro Hand simulator during the execution of a tripodal motion.

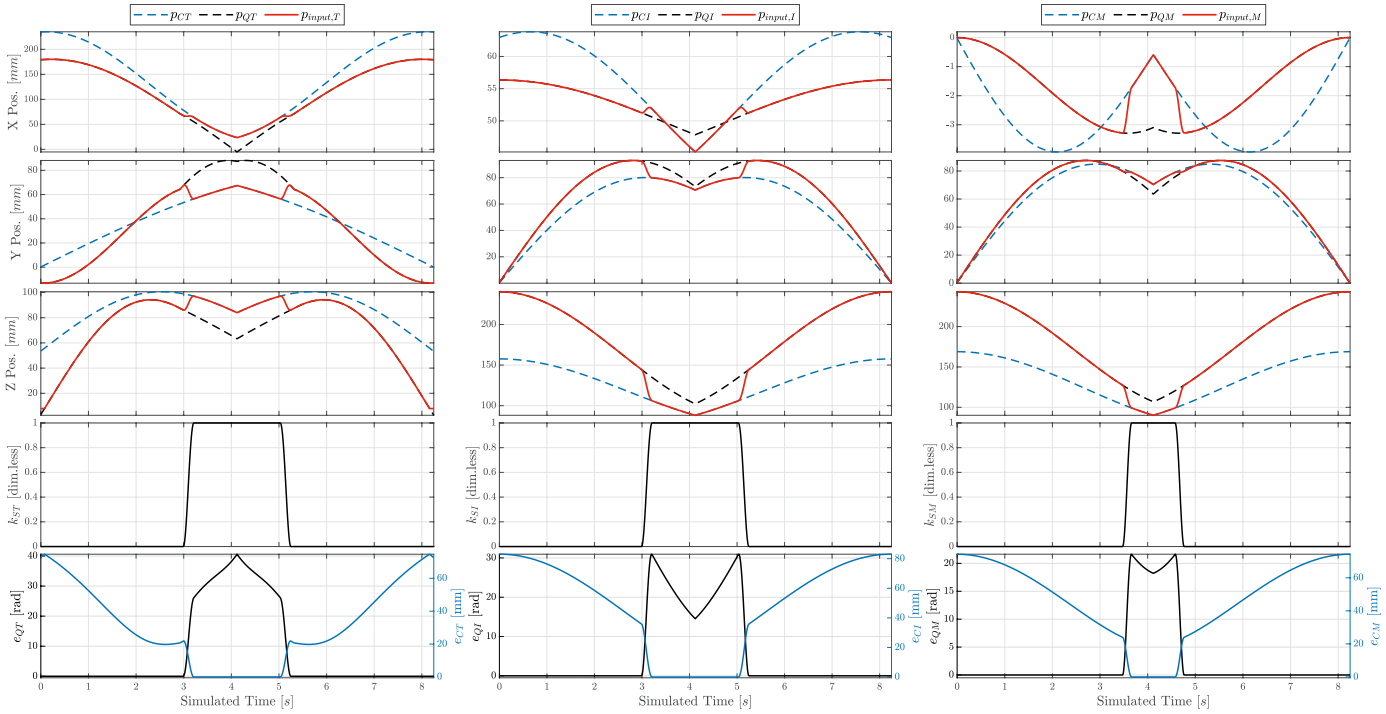

Fig. 8. Plot over time of p_C ,p_Q , p_{input}, k_S, e_Q and e_C for the thumb, index and middle fingers (columns from left to right) during the tripodal closure motion visually reported in Fig. 7.

hands with dissimilar kinematics: an approach in the object domain. *IEEE Transactions on Robotics*, 29(4), 825–837.

Kuo, L.C., Chiu, H.Y., Chang, C.W., Hsu, H.Y., and Sun, Y.N. (2009). Functional workspace for precision manipulation between thumb and fingers in normal hands. *Journal of Electromyography and Kinesiology*, 19(5), 829–839.

Liarokapis, M.V., Artemiadis, P.K., and Kyriakopoulos, K.J. (2013). Telemanipulation with the dlr/hit ii robot hand using a dataglove and a low cost force feedback device. In *21st Mediterranean Conference on Control and Automation*, 431–436. IEEE.

Malvezzi, M., Gioioso, G., Salvietti, G., and Prattichizzo, D. (2015). Syngrasp: A matlab toolbox for underactuated and compliant hands. *Robotics Automation Magazine, IEEE*, 22(4), 52–68.

Meattini, R., Benatti, S., Scarcia, U., De Gregorio, D., Benini, L., and Melchiorri, C. (2018). An semg-based human–robot interface for robotic hands using machine learning and synergies. *IEEE Transactions on Components, Packaging and Manufacturing Technology*, 8(7), 1149–1158.

Meeker, C., Rasmussen, T., and Ciocarlie, M. (2018). Intuitive hand teleoperation by novice operators using a continuous teleoperation subspace. In *2018 IEEE International Conference on Robotics and Automation (ICRA)*, 1–7. IEEE.

Palli, G., Scarcia, U., Melchiorri, C., and Vassura, G. (2012). Development of robotic hands: The ub hand evolution. In *2012 IEEE/RSJ International Conference on Intelligent Robots and Systems*, 5456–5457. IEEE.

Paulos, E. and Canny, J. (1998). Designing personal tele-embodiment. In *Proceedings. 1998 IEEE International Conference on Robotics and Automation (Cat. No. 98CH36146)*, volume 4, 3173–3178. IEEE.

WonikRobotics (2015). Allegro hand by wonik robotics. http://www.simlab.co.kr/Allegro-Hand.